Journal of Materials and Environmental Science
ISSN : 2028-2508
CODEN : JMESCN

J. Mater. Environ. Sci., 2021, Volume 12, Issue 9, Page 1243-1258

http://www.jmaterenvironsci.com

Selective and Simultaneous Removal of Methylene Blue and Cadmium (II) from Wastewater using Waste Biomass Derived Porous Carbon

Umar Yunusa[1*], Yusuf Abdullahi [2], Muhammad Garba[3], Gambo Nurudeen Bello[4], Muhammad Ahmad Aji[5], Abdulrahman Ibrahim Kubo[6]

[1] *Department of Pure and Industrial Chemistry, Bayero University, P.M.B. 3011, Kano, Nigeria*
[2] *Department of Biological Sciences, Yobe State University, P.M.B. 1144, Damaturu. Nigeria*
[3] *Department of Chemical Sciences, Federal University Kashere, P.M.B. 0182, Gombe, Nigeria*
[4] *Chemical Division, Industrial Development Department, FMITI, PMB 88, Garki 1, Abuja, Nigeria*
[5] *Department of Chemistry, School of Sciences, USCOE, P.M.B. O2, Gashua, Yobe-Nigeria*
[6] *Department of Pure and Applied Chemistry, Adamawa State University, P.M.B. 25, Mubi, Nigeria*

**Corresponding author, Email address: umaryunusa93@gmail.com*

Received 29 March 2021,
Revised 30 Sept 2021,
Accepted 1 Oct 2021

Keywords
- ✓ Adsorption,
- ✓ Porous carbon,
- ✓ *Albizia lebbeck* pods,
- ✓ Methylene blue,
- ✓ Cadmium.

umaryunusa93@gmail.com

Abstract

Since large amounts of *Albizia bebbeck* pods are abandoned in the environment, the feasibility of developing value-added products from them is of interest. In the current work, a porous carbon (denoted as ALPC) was fabricated by a one-step H_3PO_4 activation of *Albizia lebbeck* pods and applied as an adsorbent for selective and simultaneous removal of methylene (MB) and Cd^{2+} from wastewater. The characteristics of the as-prepared ALPC were examined using various techniques such as SEM, EDX, FTIR, and pH_{pzc} analyses. Results obtained demonstrated that the ALPC exhibited high removal efficiency for MB and Cd^{2+} in both single and binary systems. Noticeably, in the binary system, the adsorption capacities of MB and Cd^{2+} decreased as compared to single systems, which indicated that the adsorption system presented an antagonistic effect. Various isotherm and kinetic models were employed to elucidate the adsorption mechanisms. The experimental data fitting were consistent with the Langmuir and pseudo-second-order models, indicating a monolayered chemisorption process. The thermodynamic analysis revealed that the MB and Cd^{2+} adsorption on ALPC manifested spontaneously and the process was characterized by an endothermic behavior. Recyclability studies revealed that the ALPC was effectively regenerated using 0.05 M HNO_3 and was reused for five consecutive adsorption-desorption cycles without much loss in its initial adsorption capacity.

1. Introduction

With the rapid industrialization and urbanization, the prominent pollutants encountered in the aquatic systems are various heavy metals, dyes, pharmaceuticals, pesticides etc. In particular, dyes are normally found to coexist with heavy metal ions in industrial effluent [1]. The presence of these pollutants at elevated levels in wastewater have deleterious effects on humans and other biological systems [2]. Many technologies were developed and applied in order to minimize their contents in wastewaters, including advanced oxidation processes, biological treatment, photocatalytic degradation, ozonation and filtration [3]. However, main drawbacks of these techniques are related to energy expensiveness, low efficiency, catalyst management and residual toxicity in treated wastewaters and

resulting byproducts [4]. The adsorption approach proved to be viable alternative to remove dyes and heavy metals from wastewaters because of its simplicity, low cost and effectiveness [5].

Up to date, numerous studies were focused on mono-component adsorption of dyes and heavy metals onto various adsorbents [6,7]. However, limited data are available on multi-component adsorption. Although some studies have reported the removal of MB and Cd^{2+} from wastewater using different adsorbents including charcoal powder [8], activated carbon [9] and magnesium silicate-hydrothermal carbon composite [10], no report (to our knowledge) has been documented on simultaneous removal these pollutants using porous carbon derived from *Albizia lebbeck* pods (ALPC). Considering the coexistence of dyes and heavy metals in industrial wastewaters, the investigation of their simultaneous removal is highly imperative. Hence, the objectives of current study distributed into five parts were: (i) to fabricate a porous carbon from *Albizia lebbeck* pods using chemical activation approach; (ii) to elucidate the morphological and chemical characteristics of the as-prepared adsorbent via SEM, FTIR, Boehm titration, EDX and pH_{pzc} analyses; (iii) to assess its performance in the removal of MB and Cd^{2+} from their respective single (S) and binary (B) component solutions; (iv) to investigate the feasibility of regenerating and reusing ALPC using acidic agent as desorption medium; (v) to examined the practical potential of the ALPC for the treatment of real wastewater.

2. Experimental section

2.1 Materials and chemicals

Albizia lebbeck pods (ALP) were sourced from Yobe State, Nigeria. They were washed thoroughly with deionized water to remove impurities, and dried in oven at 105 °C for 12 h. Methylene blue ($C_{16}H_{18}ClN_3S$; CI:52015), cadmium nitrate Cd $(NO_3)_2.4H_2O$, phosphoric acid (H_3PO_4) and other chemicals employed in this study were analytical grade and acquired from Sigma-Aldrich (USA). Deionized water was used throughout the experimental process. The initial pH of the test solutions was adjusted to the preferred values with HNO_3 (0.1 M) or NH_4OH (0. 1 M).

2.2 Porous carbon preparation and characterization

The dried biomass was impregnated with a 50 wt.% H_3PO_4 solution at a ratio of 2:1 (g H_3PO_4/g dried biomass) and the mixture was kept in an ultrasonic bath for 4 h. Afterwards, the impregnated sample was carbonized in a muffle furnace (SXL-1008) at 550 °C (heating rate of 10 °C per min) for 2 h under nitrogen atmosphere. After cooling to room temperature, the sample was repeatedly rinsed to neutrality with hot deionized water and then dried at 105 °C in a vacuum oven for 24 h. The fabricated porous carbon material is hereafter denoted as ALPC. Finally, the ALPC was pulverized, sieved to desired particle size (120 µm), and kept in an airtight container for characterization and adsorption studies.

The FTIR spectra of the ALPC in the region of 4000–650 cm^{-1} were recorded with Cary 630 spectrometer (Agilent). The surface morphology of the ALPC was imaged using Phillips XL 30 scanning electron microscope. The elemental content of the ALPC was analyzed using FEI Quanta EDX Unit (FEG 650). The point of zero charge (pH_{pzc}) of ALPC was determined according to the pH drift protocol. The surface acidity and basicity were determined according to the Boehm titration procedure [11].

2.3 Solutions and adsorption experiment

The stock solutions (1000 mg/L) of MB and Cd^{2+} were prepared by dissolving the appropriate amounts of MB powder or $Cd(NO_3)_2$ in 1 L deionized water, respectively. The test solutions of desirable concentrations were prepared by serial dilution of the stock solutions. All the batch experiments for

single and binary component systems were conducted in a set of Erlenmeyer flasks (150 mL) containing 50 mL of adsorbate solution of fixed concentration (50 mg/L for MB; 100 mg/L for Cd^{2+}). The flasks were sealed with foil and agitated at 150 rpm (30 ± 1 °C) in an incubator shaker (Innova 4000; New Brunswick). To study the adsorption as a function of contact time, 5 to 150 min was considered. To evaluate the influence of initial pH, 3– 9 pH range was used. For isotherm study, the initial concentrations of each adsorbate, MB and Cd^{2+} were varied between 25–100 mg/L and 50–200 mg/L, respectively. The effect of temperature was evaluated in the range of 30-60 °C. The volume of adsorbate solution (50 mL), agitation speed (150 rpm), and adsorbent dosage (1 g/L) were kept constant in all batch experiments. After agitation for prescribed contact time, the adsorbent was separated from the aqueous phase using a membrane Millipore filter.

2.4 Regeneration and reusability of the ALPC adsorbent

The feasibility of regenerating ALPC for repeated use was investigated for five consecutive cycles using HNO_3 as the desorbing agent under the same conditions. Basically, a mass of pollutant-loaded ALPC (0.05 g) was added to flask containing 50 mL of 0.05 M HNO_3 solution. The mixture was agitated (150 rpm) at (30 ± 1 °C) for 120 min in an incubator shaker. Then the adsorbent was separated using membrane filter and then washed thoroughly with deionized water to remove the acidic agent. After washing, the sample was dried at 70 °C overnight. Finally, the dried ALPC was used in the next adsorption cycle.

2.5 Application of ALPC to real wastewater sample

A real wastewater sample was collected from a local textile industry and was employed as an adsorption medium for evaluating the practical application of ALPC in MB and Cd^{2+} removal. The wastewater sample was characterized in terms of physicochemical parameters and then subjected to MB and Cd^{2+} contamination with a concentration of 50 and 100 mg/L, respectively. The adsorption test was performed by mixing 0.05 g of the ALPC with 50 mL of the wastewater sample at natural pH of the solution (without adjustment). After agitation (150 rpm) for 120 min, the adsorbent was recovered by filtration and the residual concentration of target adsorbate in the filtrate was analyzed.

2.6 Analysis and calculation of adsorption parameters

All of the experiments were conducted in triplicate and the mean of the results were utilized for data analysis. The residual concentration of MB was analyzed using Perkin Elmer UV–visible spectrophotometer (Labda 35) at 662 nm and cadmium ions concentration was measured using a microwave plasma atomic emission spectrometer (MP-AES 4210; Agilent). Additionally, the pH of test solutions during the experiments were monitored using a pH-Meter Jenway 3510.

All the **equations** employed in the current study to evaluate the adsorption performance as well as those associated with equilibrium, kinetics and thermodynamics of MB and Cd^{2+} adsorption onto ALPC are disclosed in **Table 1**.

3. Results and Discussion

3.1 Morphological analysis

SEM was employed to examine the surface morphology of the precursor and the synthesized adsorbent as displayed in **Figure 1**. No pore was visualized on the precursor surface **(Figure 1a)** whereas the ALPC has a highly heterogeneous surface and porous structure **(Figure 1b).** High pyrolysis temperature and H_3PO_4 used for impregnation were speculated to be responsible for the pore

development in ALPC. The porous structure enhances the accommodation of adsorbate molecules on the APLC surface resulting in higher adsorption performance. **Figures 1c–d** reveal that the adsorption of MB and Cd^{2+} causes appreciable morphological changes to the surface of APLC which are reflected in the complete distortion and coverage of the pores.

Table 1. Equations used in the present study to evaluate the adsorption data [12,13]

Name	Equation	Parameters
Removal efficiency	$R\ (\%) = \left(\frac{C_o - C_{e,t}}{C_o}\right) X\ 100$	C_o (mg/L), C_e (mg/L) and C_t denote the initial, equilibrium and residual concentration of the adsorbate, respectively. V (mL) represent the volume of the adsorbate solution and m (g) denote the dose of the adsorbent.
Adsorption capacity	$q_e = \left(\frac{C_o - C_{e,t}}{m}\right) V$	
Pseudo-first-order model	$\log(q_e - q_t) = \log q_e - k_1 t$	t is the adsorption time (min); q_e and q_t (mg/g) represent the adsorption capacity at equilibrium and t time; and k_1 (min^{-1}) and k_2 (g/mg min) are the rate constants.
Pseudo-second-order model	$\frac{t}{q_t} = \frac{1}{k_2 qe^2} + \frac{t}{q_e}$	
Intraparticle diffusion model	$q_t = k_{id} t^{1/2} + C$	k_{id} is the intraparticle diffusion constant and C denotes the thickness of the boundary layer.
Langmuir isotherm	$\frac{C_e}{q_e} = \frac{1}{K_L q_m} + \frac{C_e}{q_m}$	K_L and n are measures of the adsorption intensity; q_m and K_F are associated with theoretical adsorption capacity.
Freundlich isotherm	$\log q_e = \log K_F + \frac{1}{n} \log C_e$	
Uptake capacity ratio	$R = \frac{q_{m,a\ binary}}{q_{m,a\ single}}$	$q_{ma,binary}$ and $q_{ma,single}$ denote the maximum adsorption capacity of component a in binary and single system, respectively.
Gibbs free energy	$\Delta G = -RT \ln K_d$	ΔG, ΔH, and ΔS denote the Gibbs free energy, enthalpy and entropy change, respectfully; T is temperature; R is the gas constant. K_d is an equilibrium constant.
Van't Hoff	$\ln K_d = \frac{\Delta S}{R} - \frac{\Delta H}{RT}$	

3.2 Surface chemistry and elemental composition

The surface functional groups of ALPC for pre- and post-adsorption of MB and Cd^{2+} were explored by Fourier transform infrared spectroscopy **(Figure 2).** The broad absorption band at 3361 cm^{-1}, is characteristic of the stretching vibration of hydroxyl (-OH) group. The peak had shifted to 3272 cm^{-1} and 3327 cm^{-1} after adsorption of MB and Cd^{2+}, respectively. The change in peak position clearly illustrate that the state of –OH was affected by binding with MB and Cd^{2+} [14]. The peak at 1547 cm^{-1} **(Figure 2a)** which is associated with carboxylate stretching shifted to 1514 cm^{-1} **(Figure 2b)** and 1526 cm^{-1} **(Figure 2c)**, which reveal it role in the binding of adsorbate molecules. The new peaks appearing in the range 1300 to 700 cm^{-1} **(Figures 2b-c)** suggested the successful adsorption of MB and Cd^{2+} on ALPC surface.

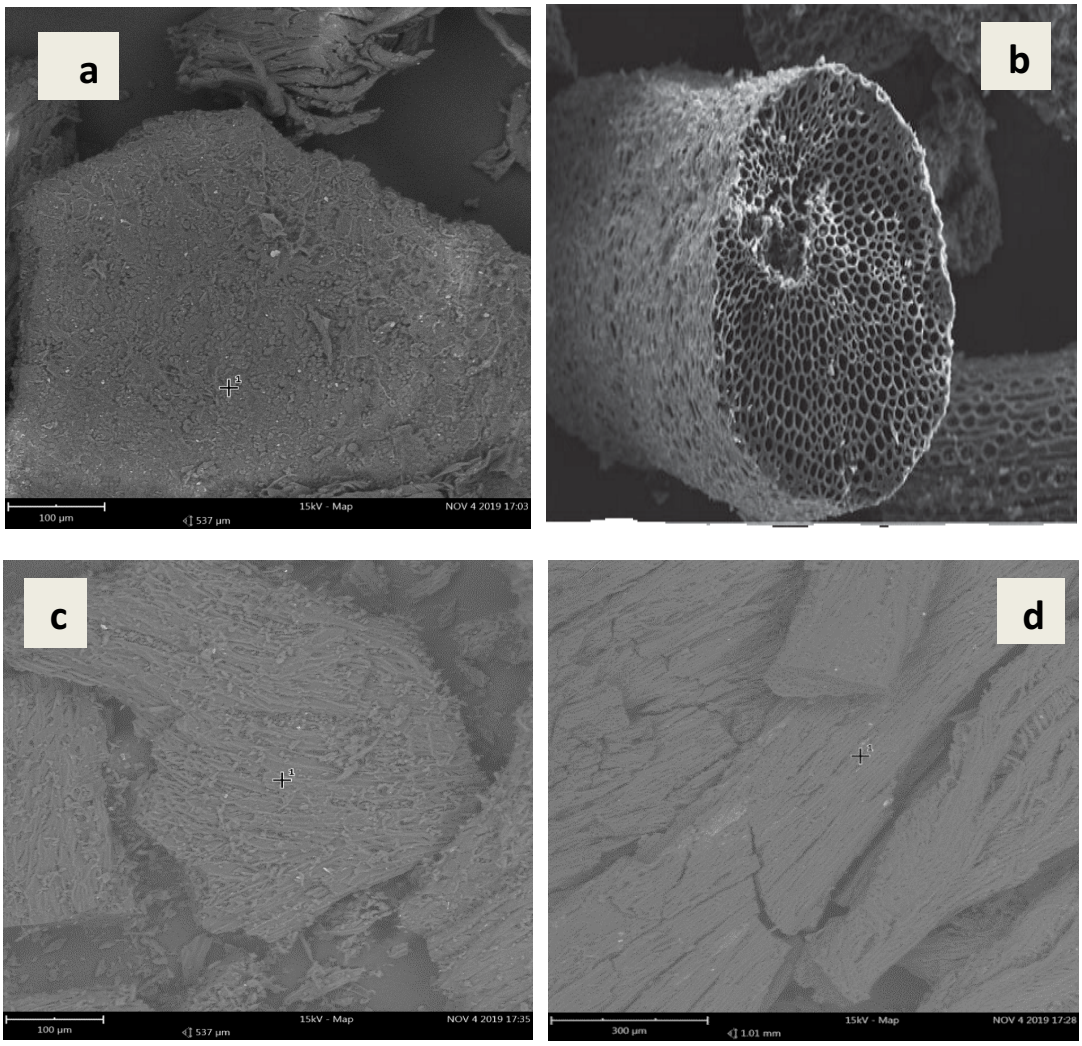

Figure 1. SEM Micrographs of (a) ALP (b) ALPC (c)ALPC/MB (c) ALPC/Cd^{2+}

Table 2 disclose quantitative information on the acidic and basic groups on the ALPC surface (obtained through Boehm titration) and the point of zero charge (pH_{pzc}). It was observed that the ALPC surface is not enriched with acidic functionalities as evidenced by the low number of carboxylic groups. Thus, the ALPC presents weak acidic character as reflected by pH_{pzc} value of 6.58.

Table 2. Content of functional groups and pH_{pzc} for ALPC

Carboxylic (mmol/g)	Phenolic (mmol/g)	Lactone (mmol/g)	Total acidity (mmol/g)	Total basicity (mmol/g)	pH_{Pzc}
0.78	0.90	0.20	1.88	1.66	6.50

Table 3 presents the elemental composition of ALP and ALPC as obtained from EDX analysis. As expected, an increase in the carbon content and a decrease in the oxygen content was observed after H_3PO_4 activation of ALP. The acid serve as a dehydrating agent promoting the volatilization of the biomass components, namely, cellulose, hemicellulose, and lignin [15]. Additionally, the EDX profile has confirmed the incorporation of elemental phosphorus (2.43%) in the biomass matrix during the H_3PO_4 activation process.

3.3 Influence of initial pH on MB and Cd^{2+} adsorption

To explore the influence of solution pH on the adsorption performance of ALPC, batch experiments were performed at pH values of 3 to 9. The removal of both MB and Cd^{2+} by ALPC was found to increase with the raising of pH values from 3─7 and remained unchanged thereafter **(Figure 3).** It is obvious that the value of removal efficiency of both MB and Cd^{2+} is not remarkably affected by the transition from the single system to the binary system. The variation in MB and Cd^{2+} removal with respect to the solution pH could be explained on the basis of the adsorbent surface charge and the adsorbate species present in solution.

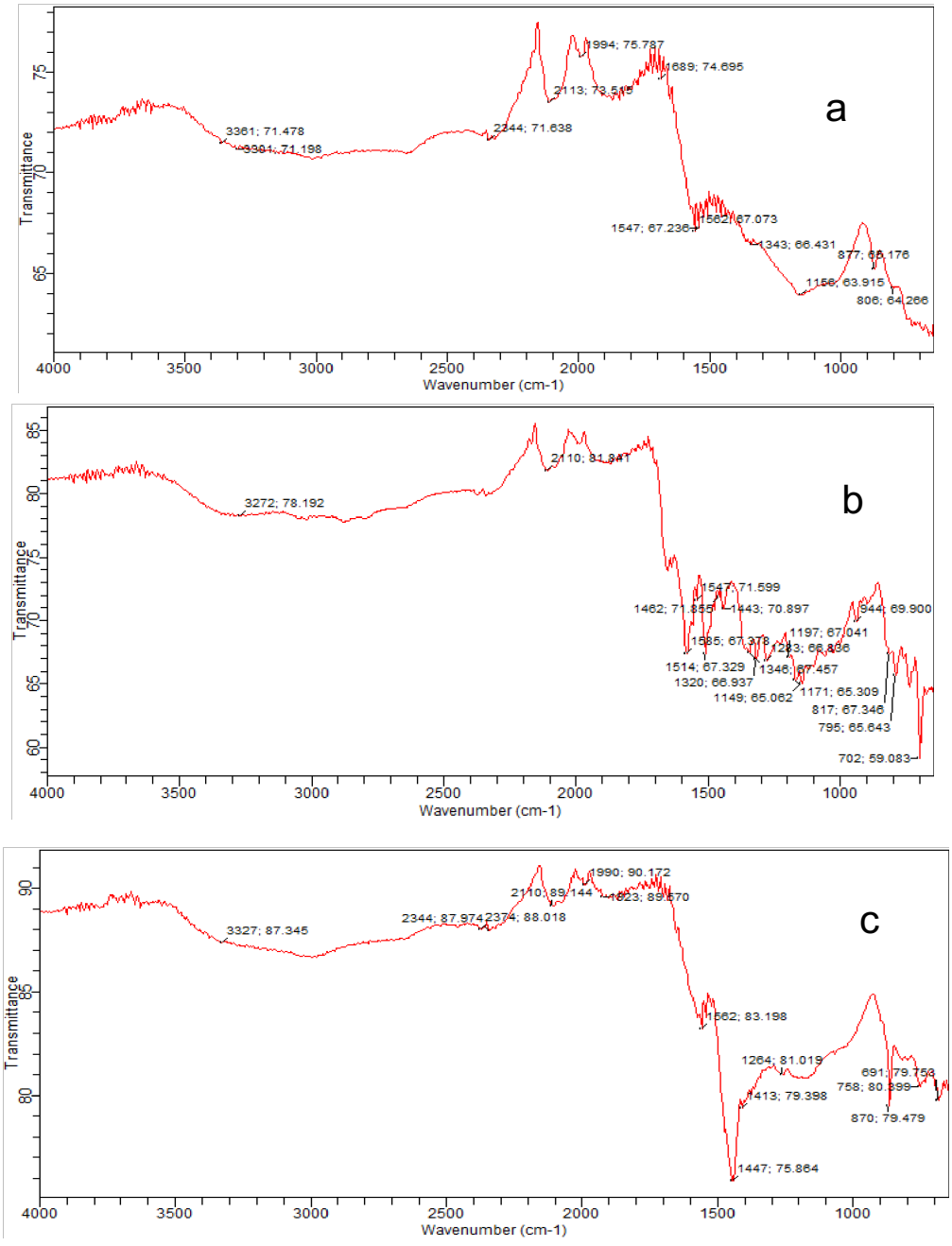

Figure 2. FTIR spectra of (a) ALPC (b) ALPC/MB (c) ALPC/Cd^{2+}

Table 3. Elemental composition of ALP and ALPC as determined by EDX analysis

Sample	C (at %)	O (at %)	S (at %)	N (at %)	P (at %)
ALP	59.10	36.72	0.22	3.96	─
ALPC	78.92	15.10	0.15	3.40	2.43

It is pertinent to state here that MB, as a cationic dye, yields positively charged ion (MB^+) in an aqueous solution. Thus, the fact that low adsorption of MB and Cd^{2+} occurred at a lower pH could be ascribed to the increase in the positive charge density of ALPC owing to protonation, which did not favor the adsorption of positively charged MB^+ and Cd^{2+} ions due to electrostatic repulsion. Furthermore, there is fierce competition at low pH values between the abundant H^+ and cationic adsorbates for available adsorption sites on ALPC surface. Additionally, the pH_{pzc} value of ALPC was 6.5 **(Table 2),** implying that ALPC bears a net negative charge at pH > 6.5, which was favorable for adsorption of cationic contaminants. This result is consistent with the trends reported in other studies [16,17]. For subsequent experiments, the pH was fixed at 7.0 for both adsorbates.

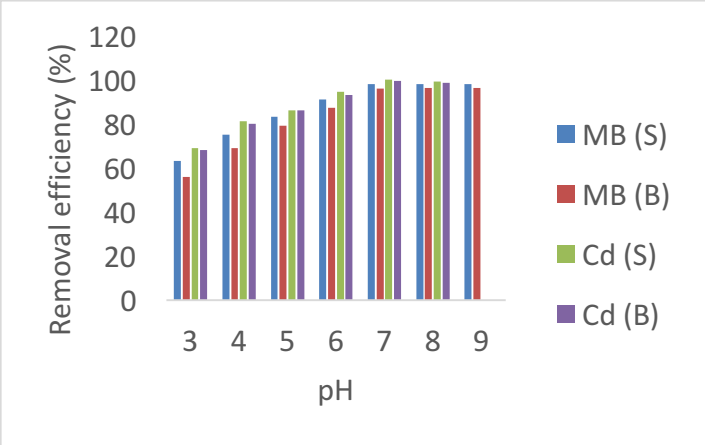

Figure 3. Influence of initial pH on removal efficiency of MB and Cd^{2+} ($C_{o,\,MB}$ = 50 mg/L, $C_{o,\,Cd}^{2+}$ = 100 mg/L, time 120 min, adsorbent dosage 1 g/L)

3.4 Adsorption kinetics

The experimental kinetic data for the adsorption of MB and Cd^{2+} by ALPC is presented in **Figure 4.** A brief look at the kinetic curve indicate that there is a gradual increase in the adsorption of adsorbates with time and apparent equilibrium was attained at around 90 min residence time on ALPC surface for both of the studied pollutants. This indicate that ALPC is characterized by a fast MB and Cd^{2+} removal capability. As displayed in **Figure 4a**, the adsorption capacity of ALPC in the binary system of MB and Cd^{2+} was compared to the values in the single system. The amount of MB adsorbed shows difference in single and binary system (48.87 and 46.1 mg/g, respectively), and, in the case of Cd^{2+}, the adsorption capacity was decreased from 97.78 to 94.1 mg/g, with an optimum contact time of 90 min.

In order to describe the adsorption rate and probable mechanism of the process, all the kinetic data obtained from experiments in the single and binary systems have been treated using various linear forms of kinetic models, viz., pseudo-first-order [18], pseudo-second-order [19], and intra-particle diffusion [20] models. The corresponding values of calculated model fitting parameters and correlation coefficients are indicated in **Table 4.** As seen, for both the adsorbates, the values of the correlation coefficient (R^2) for the pseudo-second-order model (R^2 > 0.99) were higher than those for the pseudo-first- order model. Additionally, the theoretical adsorption capacity ($q_{e,cal}$) calculated from the pseudo-second-order model was more consistent with the experimental values ($q_{e,exp}$). These signify that the adsorption kinetics is sufficiently represented by the pseudo-second-order model. Thus, we speculate that MB and Cd^{2+} adsorption by ALPC may have occurred mainly by chemisorption, which involves sharing or exchange of electrons.

The diffusion mechanism of the MB and Cd^{2+} adsorption onto ALPC was evaluated using the intraparticle diffusion model. **Figure 4b** presents the fit of the intraparticle diffusion model to the kinetic data. It was observed that the plot exhibited a non-linear trend and non-zero intercept over the whole time range. Thus, it can be inferred that intraparticle diffusion is not the sole rate controlling parameter in the adsorption process. In addition, the fact that the plot exhibited multi-linearity signifies that the adsorption of MB and Cd^{2+} on ALPC occurred in multi-step process. The first step (first 20 min) involves the diffusion of adsorbate molecules through the liquid film and are attracted to the exterior surface of the ALPC. The second step (30-60 min) represents the intraparticle diffusion stage where the Cd^{2+} and MB molecules migrate into the pores on the interior surface of the adsorbent. The third step (90-150 min), represent the final equilibrium stage where intraparticle diffusion begins to slow down due to low residual MB and Cd^{2+} concentration left in solution, enhanced electrostatic repulsion and the decreased active sites availability [21, 22].

Table 4. Kinetic parameters for MB and Cd^{2+} adsorption onto ALPC

Adsorbate		**MB (S)**	**MB (B)**	**Cd^{2+} (S)**	**Cd^{2+} (B)**
$q_{e,exp}$ (mg/g)		48.87	46.10	97.78	94.11
Pseudo-first order	$q_{e,cal}$ (mg/g)	50.91	54.48	48.42	53.59
	k_1 (min^{-1})	0.060	0.061	0.043	0.045
	R^2	0.9745	0.9400	0.9812	0.9756
Pseudo-second-order	$q_{e,cal}$ (mg/g)	47.81	50.35	100.04	99.09
	k_2 (g/mg min)	0.022	0.014	0.020	0.017
	R^2	0.9982	0.9936	0.9998	0.9996

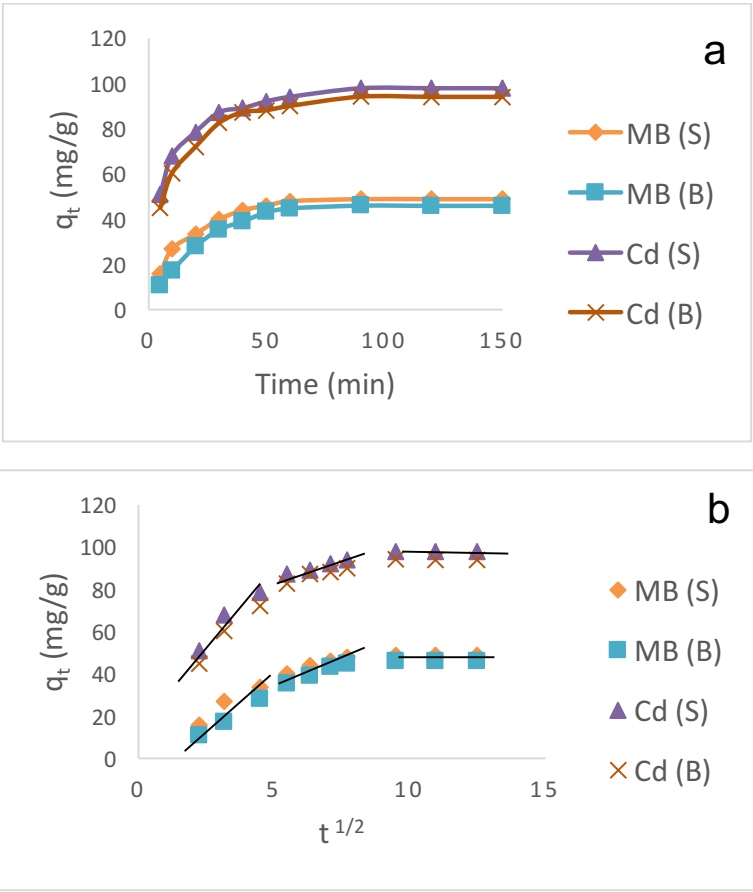

Figure 4. (a) Kinetics of MB and Cd^{2+} adsorption onto ALPC (b) Intraparticle diffusion model plot ($C_{o,\,MB}$ = 50 mg/L, $C_{o,\,Cd^{2+}}$ = 100 mg/L, pH 7, adsorbent dosage 1 g/L)

3.5 Influence of initial concentration

The initial concentration is a crucial parameter that can substantially influence the adsorption performance of a given adsorbent. The effect of the initial adsorbate concentration on adsorption capacity of ALPC in both single and binary system was investigated in the range of 25–100 mg/L for MB, and 50–200 mg/L for Cd^{2+}. As disclosed in **Figures 5a-b,** the adsorption capacity of ALPC for MB and Cd^{2+} in both single and binary mixture increases with increasing concentration of the adsorbates. This was attributed to increasing concentration gradient, which provided the required driving force to overwhelm all mass transfer resistances between the bulk liquid and adsorbent particles [23]. Moreover, high initial concentration enhances the accessibility of active sites by adsorbate molecules as well as effective electrostatic interaction at solid-liquid interface [17,24]. Comparing the profiles of the single and binary systems, the latter were always lower during the adsorption process.

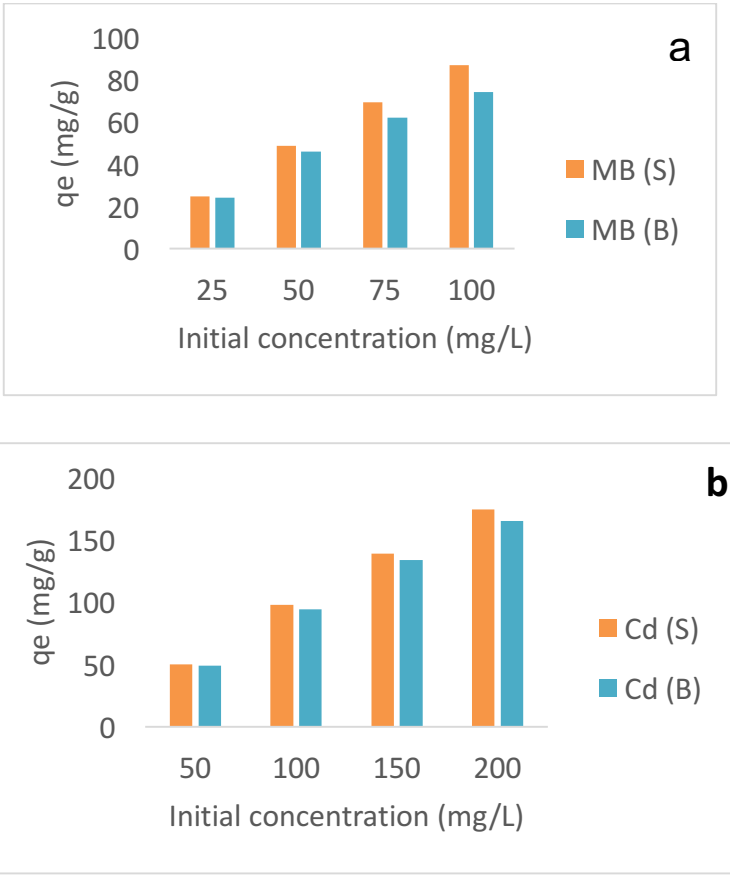

Figure 5. Influence of initial concentration on the adsorbed amount of (a) MB and (b) Cd^{2+} (time 120 min, pH 7, adsorbent dosage 1 g/L)

3.6 Adsorption isotherms

To gain insight on the distribution mechanism of the MB and Cd^{2+} on the ALPC surface, the equilibrium data for both single and binary systems were adjusted to two isothermal models, namely, Langmuir [25] and Freundlich [26]. The linear fittings of the selected isotherm models are presented in **Figures 6a-b** and the calculated fitting parameters are reported in **Table 5.** Attending to the R^2 values in **Table 5,** which are relative to the accuracy of the linear regression, one can deduce that the Langmuir model fit rather well since the corresponding regression coefficients ($R^2 > 0.99$ in all cases) were greater than those of the Freundlich model. In addition, the maximum adsorption capacities (q_m) estimated by the Langmuir isotherm for both the mono-component and binary systems were close to those obtained

experimentally. Furthermore, the values of R_L were found between 0 and 1, which implies that the adsorption of MB and Cd^{2+} onto ALPC is favorable [27]. All the above findings suggest that; (a) the ALPC surface is homogeneous; (b) the MB and Cd^{2+} adsorption on the ALPC occurs on active sites that are energetically equivalent and; (c) the adsorbed Cd^{2+} and MB molecules are organized as a monolayer.

Table 5. Isotherm parameters for MB and Cd^{2+} adsorption onto ALPC

Adsorbate	Langmuir			Freundlich		
	q_m	R_L	R^2	K_F	n	R^2
MB (S)	91.74	0.02	0.9943	58.42	7.99	0.9477
MB (B)	80.01	0.05	0.9935	27.00	3.07	0.9823
Cd^{2+} (S)	185.19	0.04	0.9923	89.43	5.29	0.9917
Cd^{2+} (B)	181.81	0.07	0.9986	51.69	3.00	0.9891

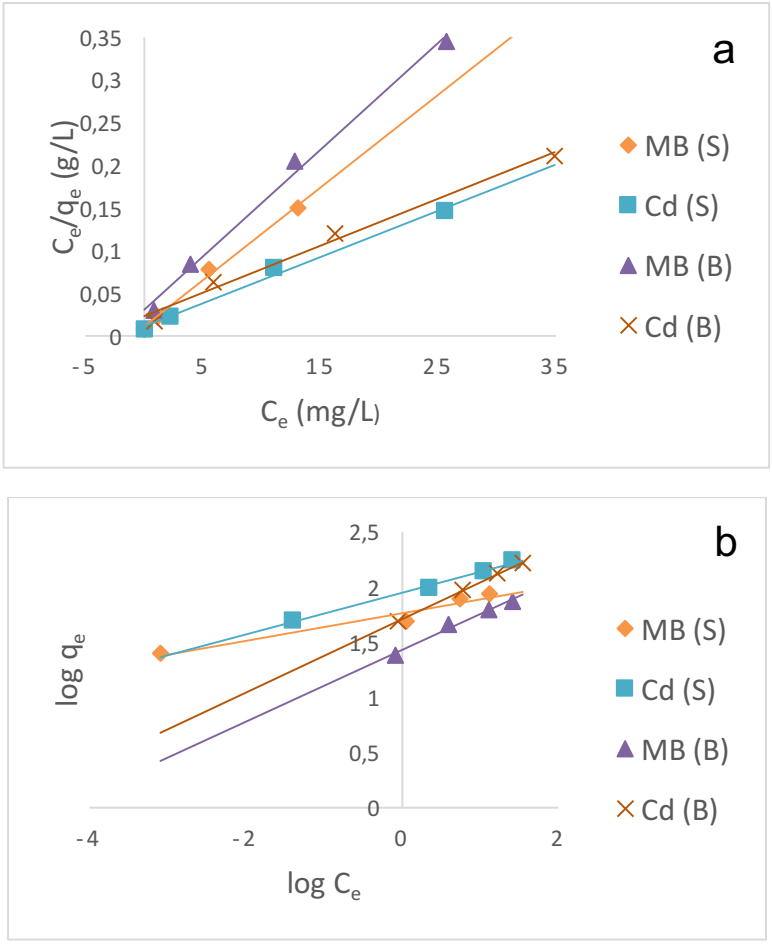

Figure 6. Isotherms plots for (a) Langmuir and (b) Freundlich models

3.7 Thermodynamic analysis

To better understand the adsorption behavior, the thermodynamic parameters such as ΔG, ΔH, and ΔS were calculated using the Gibbs energy and Van't Hoff equations. The values for the thermodynamic parameters are reflected in **Table 6.** ΔG values are negative and decrease with rising temperature, demonstrating that the uptake of MB and Cd^{2+} by ALPC occurred spontaneously and higher temperature is more favorable to the adsorption process [28]. Positive values of ΔH specify that the adsorption process is endothermic in nature and the positive values of ΔS suggested the increasing randomness at solid/liquid interface during the process of adsorption [29].

Table 6. Thermodynamic parameters for MB and Cd^{2+} adsorption onto ALPC

Adsorbate	ΔH (kJ/mol)	ΔS (kJ/molK)	ΔG (kJ/mol)		
			303 K	313 K	323 K
MB (S)	2.57	0.12	-9.487	-10.556	-11.807
MB (B)	5.03	0.18	-6.221	-8.195	-9.958
Cd^{2+} (S)	2.78	0.13	-9.552	-10.990	-11.999
Cd^{2+} (B)	4.24	0.16	-6.976	-8.523	-10.299

3.8 Interactions in the MB-Cd^{2+} binary system

Generally, the amount of solute adsorbed may increase, decrease, or remain unchanged in the presence of other component(s). The experimental data for the adsorption of both adsorbates in single and binary systems have been reported in previous sections. By comparing the uptake profiles of the single and binary systems, the former were always higher throughout the adsorption test. For instance, the maximum adsorption capacity (q_m) of ALPC for MB and Cd^{2+} in single component solution were 91.74 and 184.19 mg/g, respectively. While 80.01 mg/g and 181.81 mg/g were the maximum adsorption capacities in the binary solution, respectively **(Table 5)**. Thus, the results highlight that the adsorption capacity of the adsorbent for the target adsorbates declined in the binary system as compared to the mono-component solution. This was attributed to the fact that in the binary system, partial or total competitions between adsorbate ions for the same adsorption sites on ALPC surface occur. Besides, adsorption affinity of the adsorbent surface was mutually hampered by rivalry between MB and Cd^{2+} components for the occupation of adsorption site [30,31].

The mutual effects between each component in the binary MB─Cd^{2+} system can also be assessed by evaluating the maximum adsorption capacity ratio (R) using the formula highlighted in **Table 1.** When R > 1, the uptake of component 'a' is increased by the presence of co-existing pollutant (s) (synergism); when R <1, co-existing pollutants have suppressive effect on uptake of component 'a' (antagonism); when R = 1, the binary mixture has no effect on the adsorption of each pollutant [29,32]. The adsorption capacity ratios (R) of both MB () and Cd^{2+} were established to be 0.87 and 0.97, respectively. This indicate that in the MB─Cd^{2+} binary solution, the presence of Cd^{2+} remarkably suppressed the adsorption of MB; the same trend is also observed for Cd^{2+}, although to a lesser degree. This indicate that the MB─Cd^{2+} binary adsorption system exhibited an antagonistic effect, not synergistic adsorption. In addition, the antagonistic interaction between the MB and Cd^{2+} in the binary mixture was observed to be virtually non-existent at low initial concentration **(Figure 5).** This was attributed to the adequate number of available active sites at low adsorbate concentration which averts possible competition for adsorption sites.

3.9 Regeneration and reusability of the ALPC adsorbent

The regeneration of adsorbent after its saturation with the pollutant is one of the key parameters for its economic viability in industrial applications. In this work, the spent ALPC was regenerated using dilute HNO_3 as desorbing solution. **Figure 7** demonstrates that the adsorption capacity of ALPC after five successive adsorption–regeneration cycles was 43.01 mg/g for MB and 94.0 mg/g for Cd^{2+}. Correspondingly, the adsorption capacity of ALPC for MB and Cd^{2+} was decreased by 5.86 mg/g and 3.78 mg/g after five cycles, respectively. This result affirms that ALPC exhibited good regenerative properties and provides a basis for its practical application in wastewater treatment without significant loss in the adsorption proficiency of MB and Cd^{2+}.

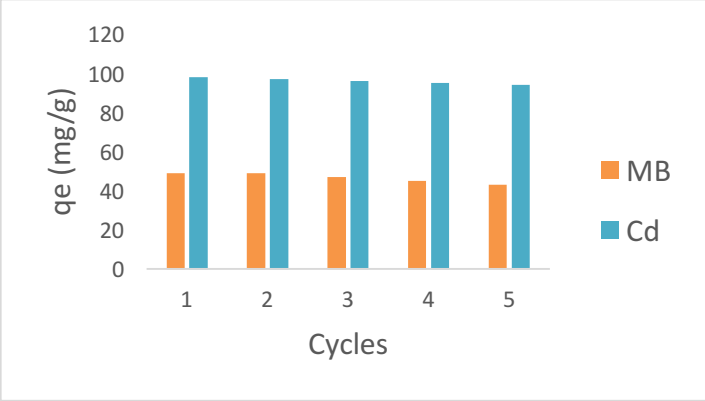

Figure 7. Adsorption-regeneration cycles of ALPC for MB and Cd^{2+}

3.10 Application of ALPC to real wastewater sample

The real wastewater sample was characterized in terms of some physicochemical parameters and the corresponding values were found to be: pH (7.7), conductivity (428 ± 0.2 µS/cm), total organic carbon (TOC) (20.4 ± 1.2 mg/L), total suspended solids (TSS) (9.22 ± mg/L), chloride (21.95 ± 2.12 mg/L), phosphate (4.55 ± 0.9 mg/L) and nitrate (17.22 ± 1.5 mg/L). In addition, Cd (1.34 ± 0.06 mg/L), Pb (1.43 ± 0.002 mg/L), Cr (0.70 ± 0.01 mg/L), Cu (0.98 ± 0.03 mg/L), and Ni (1.2 ± 0.05 mg /L) were also detected. The ALPC presented a reasonable adsorption capacity of 43.17 mg/g for MB and 94.29 mg/g for Cd^{2+} in real wastewater as compared to the 48.87 mg/g for MB and 97.78 mg/g for Cd^{2+} in deionized water system. These are corresponding to 86.34% and 94.30% removal efficiencies, respectively. The slight decrease in uptake of MB and Cd^{2+} in real wastewater was attributed to the complexity of the water matrix, which interferes with the adsorption of the target adsorbates [29]. These findings highlight the potential of ALPC in removing MB and Cd^{2+} from complex water matrices.

3.11 Comparison of ALPC with other adsorbents

The maximum adsorption capacity (q_m) gives us an insight of how efficient is certain adsorbent material if compared with other ones. Thus, to compare the adsorption performance of ALPC with other adsorbents used for MB and Cd^{2+} removal, a compilation of some tested adsorbents and their maximum adsorption capacities are disclosed in **Table 7.**

Table 7. Comparison of specific uptake of MB and Cd^{2+} on different adsorbents

Adsorbate	Adsorbent	q_m (mg/g)	References
MB	Kendu fruit peel carbon	144.4	[33]
	Iron oxide nanoparticles	91.00	[34]
	Magnetic biochar	22.88	[35]
	Almond shell	76.34	[36]
	Cellulose nanocrystals	118.0	[37]
	Polypyrrole	19.31	[38]
	Covalent organic framework	63.29	[39]
	***Albizia lebbeck* pods carbon (ALPC)**	91.74	**This work**
Cd^{2+}	*X. sorbifolia* hull carbon	388.7	[14]
	Albizia lebbeck pods	7.81	[40]
	Magnetic nanomaterial	21.58	[41]
	Modified cellulose	33.20	[42]
	T. angustifolia carbon	48.08	[43]
	Residuals nanoparticles	47.00	[44]
	Mussel shells	26.00	[45]
	***Albizia lebbeck* pods carbon (ALPC)**	185.19	**This work**

It is pertinent to note that this comparison has a relative meaning due to some factors, such as different experimental conditions (adsorbate concentration, adsorbent dosage, agitation rate, etc) and type of adsorbent material employed in each referenced study. Nevertheless, by comparing the data presented in **Table 7,** one can realize that the ALPC presented a reasonable adsorption capacity (91.74 mg/g for MB; 185.19 mg/g for Cd^{+}), which is higher than many of the reported adsorbents. This suggest that the prepared ALPC might be a potential candidate for removal of MB and Cd^{2+} from aquatic environment.

Conclusion

Porous carbon (ALPC) derived from *Albizia lebbeck* pods was successfully applied as an adsorbent for the removal of MB and Cd^{2+} in single and binary adsorption systems. The influence of process variables such as pH, initial concentration contact time and temperature were investigated using batch mode technique. The results obtained revealed that pH of 7.0 was the optimum condition for both systems and that 90 min of contact time was sufficient to attain equilibrium. In a binary system of MB─Cd^{2+}, the adsorption capacity for both MB and Cd^{2+} was lower than in single solutions. This indicate that the presence of either MB or Cd^{2+} induced an antagonistic effect on the uptake of co-existing pollutant. The equilibrium data from both single and binary system were better described by Langmuir isotherm, suggesting a monolayer adsorption process on a homogeneous surface of ALPC. The adsorption kinetics of MB and Cd^{2+} was found to conform to pseudo second-order model in both single and binary solutions. The thermodynamic analysis revealed that the uptake of MB and Cd^{2+} by ALPC occurred spontaneously and higher temperature is more favorable to the adsorption process. The adsorption-desorption results showed that ALPC had good regeneration and reusability properties. Overall, the results reflect that ALPC exhibit immense potential for the treatment of wastewater containing both MB and Cd^{2+}. For industrial application, a fixed bed column studies should be performed for scale-up and design perfection purposes.

Acknowledgement-The technical inputs of Dr. U Adam of Materials Laboratory, Leeds, are acknowledged.

Disclosure statement: *Conflict of Interest:* The authors declare that there are no conflicts of interest.
Compliance with Ethical Standards: This article does not contain any studies involving human or animal subjects.

References

1. I.A. Aguayo-Villarreal, V. Herna´ndez-Montoya, A. Bonilla-Petriciolet, R. Tovar- Go´ mez, E.M. Ramı´rez-Lo´ pez, M.A. Montes-Mora´ n, *Dyes Pigm.*, 96 (2013) 459.
2. A. Kongsuwan, P. Patnukao and P. Pavasant, *J. Ind. Eng. Chem.*, 15 (2009) 465.
3. U. Yunusa, and M.B. Ibrahim, Equilibrium and thermodynamic studies on adsorption of hexavalent chromium from aqueous solution onto low cost activated carbon, *International Journal of Engineering and Manufacturing,* 2 (2020) 52-70.
4. S.O. Ganiyu, E.D. van Hullebusch, M. Cretin, G. Esposito, and M.A. Oturan, Coupling of membrane filtration and advanced oxidation processes for removal of pharmaceutical residues: A critical review. *Sep. Purif. Technol.,* 156 (2015) 891–914.
5. U. Yunusa, B. Usman, and M.B. Ibrahim, Adsorptive removal of basic dyes and hexavalent chromium from synthetic industrial effluent: adsorbent screening, kinetic and thermodynamic studies, *International Journal of Engineering and Manufacturing,* 5 (2020) 54-74.

6. U. Yunusa, and M.B. Ibrahim, Reclamation of malachite green-bearing wastewater using desert date seed shell: adsorption isotherms, desorption and reusability studies, *ChemSearch J.,* 10 (2019) 112-122.
7. U. Yunusa, A.I. Kubo, Y. Abdullahi, T. Abdullahi, and M. Husaini, Hexavalent chromium removal from simulated wastewater using biomass-based activated carbon: kinetics, mechanism, thermodynamics and regeneration studies, *Alg. J. Eng. Tech.,* 4 (2021) 29-44.
8. Popa, N., & Visa, M. (2017). The synthesis, activation and characterization of charcoal powder for the removal of methylene blue and cadmium from wastewater. Advanced Powder Technology, 28(8), 1866–1876.
9. Nguyen, Tran, Chao, & Lin. (2019). Activated Carbons Derived from Teak Sawdust-Hydrochars for Efficient Removal of Methylene Blue, Copper, and Cadmium from Aqueous Solution. Water, 11(12), 2581.
10. Xiong, T., Yuan, X., Chen, X., Wu, Z., Wang, H., Leng, L., Zeng, G. (2018). Insight into highly efficient removal of cadmium and methylene blue by eco-friendly magnesium silicate-hydrothermal carbon composite. Applied Surface Science, 427, 1107–1117.
11. H.P. Boehm, Surface oxides on carbon and their analysis: a critical assessment, *Carbon*, 40 (2002) 145–149.
12. K.Y. Foo, and B.H. Hameed, Insights into the modeling of adsorption isotherm systems. *Chem. Eng. J.,* 156 (2010) 2-10.
13. K.L. Tan, and B.H. Hameed, Insight into the adsorption kinetics models for the removal of contaminants from aqueous solutions. *J. Taiwan Institute Chem. Eng*., 74 (2017) 25–48.
14. X. Zhang, Y. Hao, X. Wang, Z. Chen, and C. Li, Competitive Adsorption of Cadmium(II) and Mercury(II) Ions from Aqueous Solutions by Activated Carbon from *Xanthoceras sorbifolia* Bunge Hull, *J. Chem.,* (2016) 4326351.
15. A. Mokhati, O. Benturki, M. Bernardo, et al., Nanoporous carbons prepared from argan nutshells as potential removal agents of diclofenac and paroxetine, *J. Mol. Liq.,* 326 (2021) 115368.
16. X. Ma, W. Cui, L. Yang, Y. Yang, H. Chen, K. Wang, Efficient biosorption of lead (II) and cadmium (II) ions from aqueous solutions by functionalized cell with intracellular $CaCO_3$ mineral scaffolds. *Bioresour. Technol*, 185 (2015) 70-78.
17. Z.H. Khan, M. Gao, W. Qiu, Z. Song, Properties and adsorption mechanism of magnetic biochar modified with molybdenum disulfide for cadmium in aqueous solution, *Chemosphere,* 255 (2020) 126995.
18. S. Langergren, About the Theory of so-called Adsorption of Soluble Substances, *Band*. 24 (1898) 1-39.
19. Y.S. Ho, and G. McKay, Pseudo-Second-Order Model for Sorption Processes, *Proc. Biochem.,* 34 (1999) 451-465.
20. W.J. Weber, and J.C.J. Morris, Kinetics of Adsorption on Carbon from Solutions, *Sanitary Engineering Division ASCE,* 89 (1963) 31-60.
21. E. Asuquo, A. Martin, P. Nzerem, F. Siperstein, X. Fan, Adsorption of Cd (II) and Pb (II) ions from aqueous solutions using mesoporous activated carbon adsorbent: equilibrium, kinetics and characterization studies, *J. Environ. Chem. Eng.,* 5 (2017) 679–698.
22. M.C. Tonucci, L.V.A. Gurgel, S.F. de Aquino, Activated carbons from agricultural byproducts (pine tree and coconut shell), coal, and carbon nanotubes as adsorbents for removal of sulfamethoxazole from spiked aqueous solutions: kinetic and thermodynamic studies, *Ind. Crop. Prod.*, 74 (2015) 111–121.

23. J. Imanipoor, M. Mohammadi, M. Dinari, and M.R. Ehsani, Adsorption and Desorption of Amoxicillin Antibiotic from Water Matrices Using an Effective and Recyclable MIL-53(Al) Metal−Organic Framework Adsorbent, *J. Chem. Eng. Data,* https://dx.doi.org/10.1021/acs.jced.0c00736.
24. M.T. Sekulic, N. Boskovic, M. Milanovic, et al., An insight into the adsorption of three emerging pharmaceutical contaminants on multifunctional carbonous adsorbent: Mechanisms, modelling and metal coadsorption, *J. Mol. Liq.,* 284 (2019) 372-382.
25. I. Langmuir, The constitution and fundamental properties of solids and ligiuds. Part I. solids *J. Am. Chem. Soc.,* 38 (1916) 2221-2295.
26. H.M.F. Freandlinch, Uber die adsorption in losungen. Z. physical. Chemistry, *J. Phys. Chem.,* 57 (1906) 385-470.
27. N. Aarab, M. Laabd, H. Eljazouli, Experimental and DFT studies of the removal of pharmaceutical metronidazole from water using polypyrrole, *Int. J. Ind. Chem.,* 10 (2019) 269–279.
28. U. Yunusa, B. Usman, and M.B. Ibrahim, Modeling and regeneration studies for the removal of crystal violet using *Balanites aegyptiaca* seed shell activated carbon, *JOTCSA,* 8 (2021) 197-210.
29. B. Chen, W. Yue, H. Zhao, F. Long, Y. Cao and X. Pan, Simultaneous capture of methyl orange and chromium(VI) from complex wastewater using polyethylenimine cation decorated magnetic carbon nanotubes as a recyclable adsorbent, *RSC Adv.,* 9 (2019) 4722.
30. U. Yunusa, B. Usman, and M.B. Ibrahim, Experimental and quantum chemical investigation for the single and competitive adsorption of cationic dyes onto activated carbon, *Alg. J. Eng. Tech.,* 4 (2021) 7-21.
31. K. Sharma, R.K. Vyas, K. Singh, A.K. Dalai, Degradation of a synthetic binary dye mixture using reactive adsorption : Experimental and modeling studies, *J. Environ. Chem. Eng.* 6 (2018) 5732–5743.
32. V. Hern´andez-Montoya, M. A. P´erez-Cruz, D. I. Mendoza- Castillo, M. R. Moreno-Virgen and A. Bonilla-Petriciolet, *J. Environ. Manage.,* 116 (2013) 213–221.
33. S. Sahu, S. Pahi, J.K. Sahu, U.K. Sahu, and R.J. Patel, Kendu (Diospyros melanoxylon Roxb) fruit peel activated carbon—an efficient bioadsorbent for methylene blue dye: equilibrium, kinetic, and thermodynamic study, *Environ. Sci. Pollut. Res.* https://doi.org/10.1007/s11356-020-08561-2
34. S. Sharma, A. Hasan, N. Kumar, and L.M. Pandey, Removal of methylene blue dye from aqueous solution using immobilized Agrobacterium fabrum biomass along with iron oxide nanoparticles as biosorbent, *Environ. Sci. Pollut. Res*, https://doi.org/10.1007/s11356-018-2280-z.
35. M. Ruthiraan, E.C. Abdullah, N.M. Mubarak, and S. Nizamuddin, Adsorptive Removal of Methylene Blue Using Magnetic Biochar Derived from Agricultural Waste Biomass: Equilibrium, Isotherm, Kinetic Study. *Int. J. Nanoscience,* 17 (2018) 1850002.
36. C. Duran, D. Ozdes, A. Gundogdu, and H.B. Senturk, Kinetics and Isotherm Analysis of Basic Dyes Adsorption onto Almond Shell (Prunus dulcis) as a Low Cost Adsorbent, *J. Chem. Eng. Data*, 56 (2011) 2136–2147.
37. R. Batmaz, et al., Cellulose nanocrystals as promising adsorbents for the removal of cationic dyes, *Cellulose*, 21 (2014) 1655–1665.
38. M. Maruthapandi, et al., Kinetics, Isotherm, and Thermodynamic Studies of Methylene Blue Adsorption on Polyaniline and Polypyrrole Macro−Nanoparticles Synthesized by C-Dot-Initiated Polymerization, *ACS Omega*, 3 (2018) 7196−7203.

39. O. Rahmanian, M. Falsafin, and M. Dinari, High surface area benzimidazole based porous covalent organic framework for removal of methylene blue from aqueous solutions, *Polym Int*, 69 (2020) 712–718.
40. S. Mustapha, D.T. Shuaib, M. M. Ndamitso, et al., Adsorption isotherm, kinetic and thermodynamic studies for the removal of Pb(II), Cd(II), Zn(II) and Cu(II) ions from aqueous solutions using *Albizia lebbeck* pods, *Appl. Water Sci.,* 9 (2019) 142.
41. T. Lei, S. Li, F. Jiang, et al., Adsorption of Cadmium Ions from an Aqueous Solution on a Highly Stable Dopamine-Modified Magnetic Nano Adsorbent, *Nanoscale Res. Lett*. 14 (2019) 352.
42. A. Daochalermwong, N. Chanka, K. Songsrirote, Removal of Heavy Metal Ions Using Modified Celluloses Prepared from Pineapple Leaf Fiber, *ACS Omega*, 5 (2020) 5285−5296.
43. C. Tang, Y.Shu, R. Zhang, et al., Comparison of the removal and adsorption mechanisms of cadmium and lead from aqueous solution by activated carbons prepared from *Typha angustifolia* and *Salix matsudana, RSC Adv.,* 7 (2017) 16092.
44. E. Elkhatib, A. Mahdy, F. Sherif, W. Elshemy, Competitive adsorption of cadmium(II) from Aqueous Solutions onto Nanoparticles of Water Treatment Residual, *J. Nanomaterials,* (2016) 8496798.
45. H.T. Vana, L.H. Nguyenb, V.D. Nguyenc, Characteristics and mechanisms of cadmium adsorption onto biogenic aragonite shells-derived biosorbent: Batch and column studies, https://doi.org/10.1016/j.jenvman.2018.09.079.

(2021) ; http://www.jmaterenvironsci.com